

## Detecting translocation of individual single stranded DNA homopolymers through a fabricated nanopore chip

Young-Rok Kim,<sup>1</sup> Chang Ming Li,<sup>2</sup> Qiao Wang<sup>3</sup>, Peng Chen<sup>2</sup>

<sup>1</sup> Samsung Advanced Institute of Technology, South Korea, <sup>2</sup> Division of Bioengineering, School of Chemical and Biomedical Engineering, Nanyang Technological University, Singapore, <sup>3</sup> Department of Radio Engineering, Southeast University, China

### TABLE OF CONTENTS

1. Abstract
2. Introduction
3. Methods and Materials
  - 3.1. Nanopore fabrication
  - 3.2. Experimental setup and data acquisition
  - 3.3. Solutions and molecules
4. Results
5. Conclusion and discussion
6. Acknowledgement
7. References

## 1. ABSTRACT

Fabricated solid-state nanopore chips are used to probe individual single stranded DNA (ssDNA) homopolymers. Based on the analysis of the current blockage caused by DNA translocation through a voltage-biased nanopore, we discovered that the hydrodynamic diameter of ssDNA homopolymer helix is comparable to that of double stranded DNA (dsDNA) helix. This proof-of-principle demonstration shows that solid-state nanopore technology can be used to spy on secondary structures of biopolymers. We also show that ssDNA manifests slower and distinct translocation kinetics in comparison to dsDNA. Furthermore, the present study helps to refine our understanding of the ssDNA translocation kinetics through narrower alpha-hemolysin protein pores.

## 2. INTRODUCTION

The convergence of biotechnology and nanotechnology is bringing tremendous opportunities to biological science in terms of developing more sensitive, faster, cheaper, novel bio-devices at nanometer scale. As a recent example, nanopores that reside within an insulating thin membrane have been used as ultimate bio-analytical devices, i.e., single molecule sensors. Nanopore technologies have drawn much attention from experimental or theoretical perspectives due to the unique and vast potentials in rapid single molecule characterization, polymer (e.g. DNA) sequencing, and diagnosis of diseases (1-10). Such single-molecule approach makes it possible to explore individual molecular details that are obscured in ensemble-average measurements. At the same time, the

speed and ease with which molecules can be captured and sensed by a nanopore make it possible to achieve very high through-put and allow one to examine the heterogeneity and distribution of molecular properties from a population of molecules.

Biological protein pores or channels, such as alpha-hemolysin that self-assembles into lipid bilayer with remarkable fidelity and reproducibility to form a nanopore with the limiting aperture of ~1.5 nm, were first used to detect individual polymers such as single stranded DNA (ssDNA) or RNA (4,6,11-13). The ability of biological nanopores to detect polymer size, copy number, hybridization, phosphorylation state, and composition difference demonstrates the exquisite sensitivity of a nanopore device and its promise for novel applications (3,6-8,10,13,14). The recent discovery that alpha-hemolysin nanopore can recognize ssDNA with single nucleobase resolution strengthens the hope for its utility in rapid DNA sequencing (15).

Whereas the fixed aperture size, delicate physical, chemical, mechanical and electrical properties of protein nanopores greatly limit the range of analytes and the repertoire of experimental possibilities. To overcome these limitations, single artificial nanopores in robust, inorganic thin membranes have recently been fabricated and drawn increasing interests. Nanopores embedded in silicon dioxide membrane have been created using high energy electron beam in Transmission Electron Microscope with direct visual feedback for the size control (16). Alternatively, single digit nanometer pores have been fabricated on silicon nitride membrane using feedback controlled ion beam sculpting technique(17). However, the ion beam, electron beam, or chemical etch fabrication conditions used to create nanopores usually yield uncharacterized and possibly unfavorable surface properties that can interfere with the pore's sensing capabilities. A strategy of using atomic layer deposition has been developed to fine-tune nanopore size with Angstrom precision, and to coat the nanopore with desired dielectric materials such as alumina leading to higher sensing throughput and lower noise level (18).

Solid-state nanopores have been employed to probe double stranded DNA molecules (dsDNAs) which are too large in cross-sectional diameter (~ 2.4 nm) to pass through and be examined by a narrow alpha-hemolysin pore. Negatively charged DNA molecule can be electrophoretically driven through a voltage biased nanopore and its translocation yields a temporary blockage of ionic current that otherwise flows unimpeded through an open nanopore. Such transient current signal reveals the presence and properties of the translocating molecule. As demonstrated previously (19), the current blockage level caused by DNA translocation is given by:  $I_{\text{block}} \propto A \times V_{\text{bias}}/L_{\text{pore}}$ , where  $V_{\text{bias}}$  is the applied voltage,  $L_{\text{pore}}$  the effective pore length, and  $A$  the hydrodynamic cross section of the translocating molecule. And the translocation kinetics of dsDNA can be described by a rapid free electrophoretic motion disturbed by random walk. The

translocation velocity is linearly proportional to the applied voltage bias.

In this contribution, we studied the electrophoretic transport of ssDNA homopolymers through synthesized nanopores with thin alumina coating by atomic layer deposition. In direct comparison with dsDNA translocation, we present that ssDNA manifests slower and distinct translocation kinetics and its secondary helical structure can be revealed based on its current blockage level. Furthermore, the results help to refine our understanding of the ssDNA translocation kinetics through narrower alpha-hemolysin protein pores.

### 3. METHODS AND MATERIALS

#### 3.1. Nanopore fabrication

Nanopores were fabricated in  $25\ \mu\text{m} \times 25\ \mu\text{m}$ , free-standing, stoichiometric, low-pressure chemical vapor deposited, ~200 nm thick  $\text{Si}_3\text{N}_4$  membranes that were supported on a  $12\ \text{mm} \times 6\ \text{mm} \times 0.4\ \text{mm}$  N-type, phosphorus doped, silicon substrate (100) frame. First, a 70 - 100 nm pore was drilled at the center of this membrane using a focused ion beam machine (FIB, Micron 9500). This large pore was subsequently sculpted using a 3 keV  $\text{Ar}^+$  ion beam reaching a final size of 5-10 nm, during which process the pore size was continuously monitored by counting the  $\text{Ar}^+$  flux through the pore (17). The  $\text{Ar}^+$  ion beam stimulated lateral atomic flow of  $\text{Si}_3\text{N}_4$  to create a thin film of  $\text{Si}_3\text{N}_4$  material that defines a nanopore at one end of the cylindrical FIB pore.

Finally, the sculpted nanopore was coated with  $\text{Al}_2\text{O}_3$  layer, to achieve desired final pore size and minimum surface charge at solution condition we used (pH 8.0), using atomic layer deposition (ALD) procedure. ALD was carried out in a flow reactor at 225 °C using electronically controlled valves as previously reported. To generate reactive hydroxylated surfaces, all samples were treated by UV/ozone for 10 minutes immediately before placement in the flow reactor. Metal precursor, trimethylaluminum [ $\text{Al}(\text{CH}_3)_3$ ], was purchased from Aldrich Chemical Co. Water vapor was used as the oxygen source to form  $\text{Al}_2\text{O}_3$ . The alumina layer improves nanopore performance by enhancing the DNA capture rate, reducing electrical noise, controlling final pore size with Angstrom precision.

#### 3.2. Experimental setup and data acquisition

The solution on top of the nanopore (*cis* side) was confined either by a small chamber made of poly(dimethylsiloxane) (PDMS) or a glass capillary tube equipped with a grounding Ag/AgCl electrode. The circuit was completed by a positively biased Ag/AgCl electrode in a PDMS chamber (*trans* side) underneath the nanopore chip. The current through the nanopore was monitored at a 10  $\mu\text{s}$  sampling rate with low-pass filtering at 10 kHz using an Axopatch 200B amplifier (Axon Instruments, Foster City, CA). Data analysis was implemented in MATLAB (The Mathworks, Natick, MA) using custom built software routines.

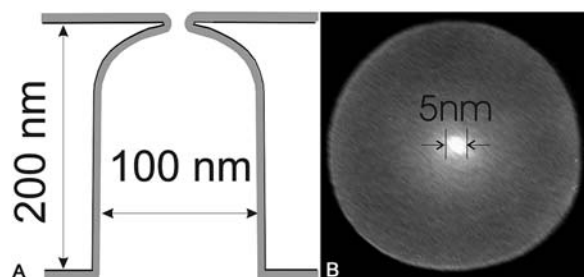


**Figure 1.** A fabricated nanopore. (a) schematic representation of its cross section. The  $\text{Al}_2\text{O}_3$  layer coated by atomic layer deposition is shown in gray. (b) top view by transmission electron microscopy.

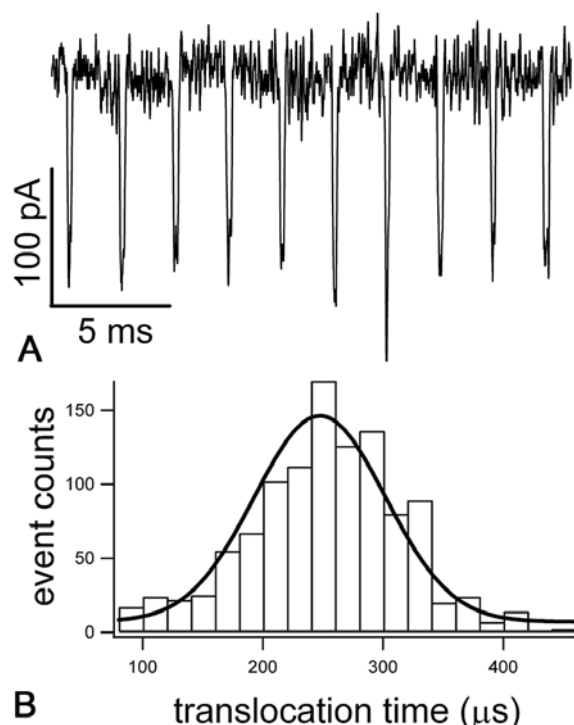


**Figure 2.** Translocation of double stranded 10 kbp DNA at driving voltage of 200 mV. (a) typical translocation events. (b) histogram of translocation time from 1093 events, fitted by a Gaussian with the peak at 247  $\mu\text{s}$ .

### 3.3. Solutions and molecules

To record DNA translocation, 5  $\mu\text{g}/\text{ml}$  DNA molecules was added to the *cis* side of the nanopore. Single stranded poly-deoxyadenosine (polydA) and poly-deoxycytosine (polydC) of 100-nucleotide-long, dA100 and dC100, were obtained from the Midland Certified Reagent Company (Midland, TX). 100 bp dsDNA was prepared from 100 bp DNA ladder (New England Biolabs, Beverly MA). KBA, a closed circular 10 kbp DNA plasmid, was linearized by digestion with *SmaI* to produce the 10 kbp dsDNA. All DNA molecules were purified after agarose gel electrophoresis using QIAquick gel extraction kit (QIAGEN, Valencia, CA). DNA molecules were stored as dried pellets at 4  $^{\circ}\text{C}$  and resuspended in TE buffer prior to

use. The TE buffer contained 1 M KCl, 10 mM Tris, 1 mM EDTA and titrated to pH 8.0.

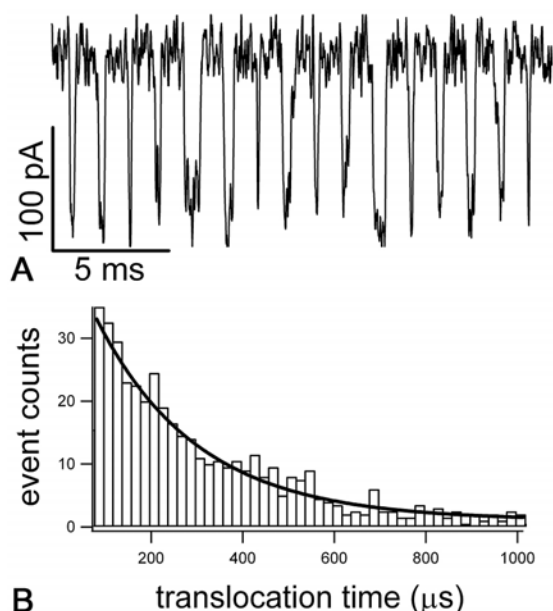
## 4. RESULTS

Figure 1A illustrates schematic representation of the cross section of a nanopore chip. A thin alumina layer coated by atomic layer deposition is shown in gray. It conformally covers uncharacterized and negatively charged pore surface. As demonstrated earlier (18), the alumina coating gives a neutral surface charge in our solution condition (pH 8.0) ensuring high capture rate of DNA molecules and lowers the noise level. The top is *cis* side where we introduce DNA molecules onto. An ionic current and DNA attracting electrical field in the pore vicinity are established when a positive voltage is applied on *trans* side with reference to the grounded *cis* side. Highly intensive electrical field near the pore entrance captures DNA molecules that diffuse into the pore vicinity and transmits them through the pore rapidly. Each DNA translocation event can be registered by a temporary current reduction signal. Figure 1B shows the transmission electron micrograph of a 5 nm pore (top view). We used pore sizes ranging from 4 - 8 nm.

As presented in our previous work (19), the highly nonlinear electrical gradient near the pore stretches randomly coiled DNA molecules, and translocates DNA molecules less than 10 kbp long in a single file fashion. Longer molecules such as bacteriophage lamda dsDNA (48.5 kbp) sometimes produce digitized current blockage levels when the translocating molecules are not fully stretched and fold to themselves. We did not observe multiple current blockages (or folded events) from the short single stranded DNA homopolymers or from the majority (> 95%) of double stranded 10 kbp DNAs used in this study.

Translocation events of 10 kbp dsDNA driven by a 200 mV voltage bias through a 4 nm pore is presented in figure 2A. The average current blockage is 135.8  $\pm$  18.8 pA (1093 events). The translocation time histogram can be fitted by a Gaussian curve (figure 2B), the peak of which indicates the average duration corresponding to a speed of 40 bp /  $\mu\text{s}$ . This data agrees with the previous experiments and predicts that, 100 bp dsDNA molecules only take about 2  $\mu\text{s}$  to pass through, too fast to be reported by our 10 kHz filtered data acquisition system. Indeed, we were not able to detect any translocations from 100 bp dsDNA (data not shown).

But surprisingly, we observed translocation signals of homopolymeric ssDNA 100mers. Figure 3A depicts translocation events from poly-deoxyadenosine 100 mers (dA100) through the same pore in figure 2. Despite the similarity in physical length ( $\sim$ 38 nm), ssDNA obviously translocates in a much slower rate in comparison to its double stranded counterpart. The translocation time histogram of dA100 molecules is shown in figure 3B. It can be fitted by a single exponential with a time constant of 228  $\mu\text{s}$ , without a well-defined peak as in the case of dsDNA (Figure 2). Translocation of poly-deoxycytosine 100mers



**Figure 3.** Translocation of single stranded dA100 at 200 mV. (a) translocation events. (b) histogram of translocation time from 947 events, fitted by an exponential with a time constant of 228  $\mu$ s.

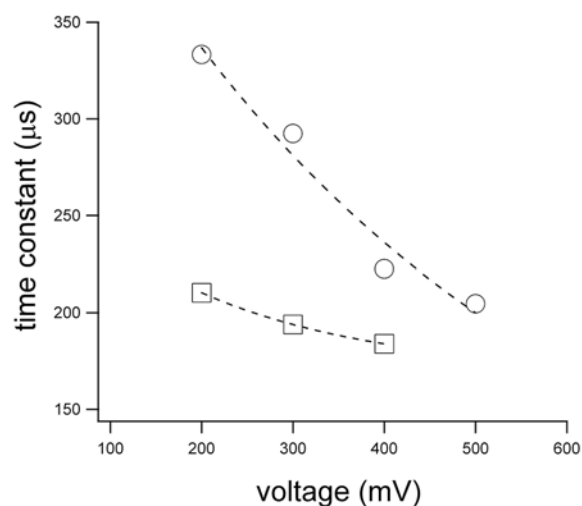


**Figure 4.** Translocation time constant of ssDNA is inversely dependent on the driving voltage. The data is collected from a 7 nm pore. Circles represent translocation time constants of dA100 at various voltages. Squares are time constants of dC100. Dotted lines are exponential fittings to illustrate trends.

(dC100) manifested similar kinetics, but with a faster time constant of 138  $\mu$ s. Translocation time constant of homopolymeric oligonucleotides showed an exponential Arrhenius-like dependence on driving voltage (figure 4, data is collected from a 7 nm pore). Such kinetics can be described by the first-order transition characterized by a single rate constant, implying that translocating ssDNA molecule experiences a single energy barrier.

Surface electrostatic charge and electro-osmotic flow may impose such an energy barrier to slow down ssDNA electrophoretic motion. In addition, theoretical studies (20,21) and experimental evidence suggest (22) that hydrophobic interaction of DNA bases and the pore surface can greatly slow down translocation of ssDNA. Furthermore, excessive counterion condensation on ssDNA (23) significantly reduces its effective charge, therefore electrophoretic force may lose its dominance over the energy barrier experienced by the translocating ssDNA molecule.

Heng *et al* (22) have studied ssDNA translocation through nanopores on thin SiO<sub>2</sub> membrane and as small as 1-3 nm. In their study, the duration, shape, and magnitude of the blocking current vary stochastically. In contrast, we observed distinct, two-level transitions between an open pore current and a well-defined blockage level from the translocating ssDNA homopolymer. The current blockage of dA100 is 120.3  $\pm$  15.0 pA (947 events) as shown in figure 3A. At first glance, this result seems to be mysterious in that the physical size of ssDNA is half of that of dsDNA yet they produce similar current blockage. But it should be pointed out that current blockage level is determined by the hydrodynamic cross-section of the translocating molecule. The translational hydrodynamic size of the molecule corresponds to a hypothetical cylinder that is impermeable to ion flows. It depends not only on molecule's physical size but also its structure and associated hydration layer.

Single stranded homopolymeric nucleic acid is known to assume secondary helical structure, which is stabilized by aromatic base stacking between two consecutive bases along the string. X-ray scattering studies showed that in water the helical radius of RNA homopolymer poly-adenosine (polyA) is 10.7 Å (24), 89% of the radius of dsDNA helix which is 12 Å (25). PolydA presumably has similar helical structure as its RNA counterpart, but its exact structural information from similar X-ray studies is absent. In high salt concentration, such as 1M KCl used in our experiments, base stacking is dominant and determines the ssDNA helical structure, because the competing electrical repulsion between phosphate groups vanishes to an insignificant level because of charge screening. Under such circumstances, ssDNA helix is supposed to have coiled conformation resulting in a hydrodynamic structure with much greater radius than the molecule's linear form. Poly-deoxycytosine (dC100) produced current blockage of 97.3  $\pm$  13.4 pA (257 events) from the same pore in figure 2, less than the current blockage caused by dA100. It is consistent with the previous finding on RNA homopolymers that polyC assumes smaller helix comparing to polyA (26).

If the translocation events observed from the ssDNA oligomers are due to ssDNA-nanopore interaction, how such interaction affect the current blockage (or molecule's hydrodynamic diameter) needs further investigation. We also observed some "sticky" or slow events (<2%) from long dsDNAs (10 kbp and 50 kbp), presumably also due to molecule-nanopore interaction. But

those sticky events showed similar current blockage with normal free-passage events (data not shown). It implies that interaction with nanopore may have negligible effects on molecule's double helical structure therefore its translational hydrodynamic diameter.

### 5. CONCLUSION AND DISCUSSION

Understanding ssDNA translocation through synthesized nanopores is important to the development of nanopore chip-based bio-analytical techniques such as a DNA sequencing device. It is also relevant to fundamental biological processes such as gene transfer and RNA transport through nuclear pore complex. In summary, we studied the translocation of oligonucleotide homopolymer through synthesized  $\text{Si}_3\text{N}_4$  nanopores with thin  $\text{Al}_2\text{O}_3$  coating and with a final size varying from 4 - 8 nm. Our observations (reproducible in pore size range that we used) indicated that single stranded oligonucleotide homopolymers have distinct translocation kinetics compared to that of dsDNA. In the former case, molecule movement is apparently hindered by certain energy barrier, and therefore is several orders slower than the rapid electrophoretic free-passage of dsDNA. The translocation time of the ssDNA homopolymer is exponentially distributed with a time constant (228  $\mu\text{s}$ , for dA100 at 200 mV), interestingly, comparable to the average time of its translocation through an alpha-hemolysin protein pore (330  $\mu\text{s}$ , for dA100 at 120 mV) (6). But the translocation time distribution from biopores manifested a well-defined peak and is shaped as a slightly-skewed Gaussian curve.

We demonstrated that nanopore chip technology can be used to spy on the secondary structures of single molecules. Our data suggest that ssDNA homopolymers assume helical structures. The hydrodynamic diameter of single stranded polydA is about 88.4% of double helical structure of dsDNA based on the average blockage current produced by these two types of molecules. It corresponds to a diameter of  $\sim 2.1$  nm, larger than the alpha-hemolysin aperture  $\sim 1.5$  nm. It means single stranded polydA helix has to be sequentially disrupted in order to pass through. It explains the slow kinetics observed from alpha-hemolysin experiments in contrast to the previous interpretation (27) that DNA translocation is slowed by its entropic effect. We did not identify appreciable entropic effect imposed to the rapid translocation of long dsDNA random coils.

To reveal sequential molecular or atomistic information along the nucleic acid strand using nanopores, it is desirable in many cases to denature the secondary structure of the molecule by high temperature or high pH. A recent experiment (28) demonstrated that ssDNA molecules, that denatured from natural dsDNA at pH 13 and lacking of helical structures, produced about half of the current blockage of the parent dsDNA molecules. This experiment further supports the notion that the "unexpected" "large" current blockage from ssDNA homopolymers as observed in our study is due to molecule's helical secondary structure.

### 6. ACKNOWLEDGEMENT

We acknowledge the help from Eric Brandin and Prof. Daniel Branton at Harvard University. This research was supported by URC/AcRF grant (RG 41/05) and NTU Start-up Grant to PC, NSF of China (No.60472055) to QW.

### 7. REFERENCES

1. Akeson, M., D. Branton, J. J. Kasianowicz, E. Brandin & D. W. Deamer: Microsecond time-scale discrimination among polycytidylic acid, polyadenylic acid, and polyuridylic acid as homopolymers or as segments within single RNA molecules. *Biophysical J.* 77, 3227-3233 (1999)
2. Gu, L.-Q., O., Braha, S. Conlan, S. Cheley & H. Bayley: Stochastic sensing of organic analytes by a pore-forming protein containing a molecular adapter. *Nature* 398, 686-690 (1999)
3. Howorka, S., S. Cheley & H. Bayley: Sequence-specific detection of individual DNA strands using engineered nanopores. *Nature Biotechnology* 19, 636-639 (2001)
4. Kasianowicz, J. J., E. Brandin, D. Branton. & D. W. Deamer: Characterization of individual polynucleotide molecules using a membrane channel. *PNAS* 93, 13770-13773 (1996)
5. Kullman, L., M. Winterhalter & S. M. Bezrukov: Transport of maltodextrins through maltoporin: A single-channel Study. *Biophysical J.* 82, 803-812 (2002)
6. Meller, A., D. Branton, E. Brandin, L. Nivon & J. Golovchenko: Rapid nanopore discrimination between single polynucleotide molecules. *PNAS* 97, 1079-1084 (2000)
7. Wang, H., J. E. Dunning, A. P.-H. Huang, J. A. Nyamwanda & D. Branton: DNA heterogeneity and phosphorylation unveiled by single-molecule electrophoresis. *PNAS* 101, 13472-13477 (2004)
8. Sutherland, T. C., Y.-T. Long, R.-I. Stefureac, B.-A. Irene, H.-B. Kraatz & J. S. Lee: Structure of peptides investigated by nanopore analysis. *Nano Letters* 4, 1273-1277 (2004)
9. Li, J., M. Gershow, D. Stein, E. Brandin & J. A. Golovchenko: DNA molecules and configurations in a solid-state nanopore microscope. *Nature Materials* 2, 611-615 (2003)
10. Sauer-Budge, A. F., J. A. Nyamwanda, D. K. Lubensky & D. Branton: Unzipped kinetics of double-stranded DNA in a nanopore. *Physical Review Letters* 90, 238101-238104 (2003)
11. Deamer, D. W. & D. Branton: Characterization of nucleic acids by nanopore analysis. *Accounts of Chemical Research* 35, 817-825 (2002)
12. Gu, L.-Q., S. Cheley & H. Bayley: Capture of a single molecule in a nanocavity. *Science* 291, 636640 (2001)
13. Vercoutere, W., W.-H. Stephen, H. Olsen, D. Deamer, D. Haussler & M. Akeson: Rapid discrimination among individual DNA hairpin molecules at single-nucleotide resolution using an ion channel. *Nature Biotechnology* 19, 248-252 (2001)
14. Jorge, S.-Q., A. Saghatelian, S. Cheley, H. Bayley & G. M. Reza: Single DNA rotaxanes of a transmembrane pore protein. *Angew. Chem. Int. Ed* 43, 3063-3067 (2004)

15. Ashkenasy, N., J. Sanchez-Quesada, H. Bayley & M. R. Ghadiri: Recognizing a single base in an individual DNA strand: a step toward DNA sequencing in nanopores. *Angew. Chem. Int. Ed* 44, 1401-1404 (2005)
16. Storm, A. J., J. H. Chen, X. S. Ling, H. W. Zandbergen & C. Dekker: Fabrication of solid-state nanopores with single-nanometre precision. *Nature materials* 2, 537-540 (2003)
17. Li, J., D. Stein, C. McMullan, D. Branton, M. J. Aziz & J. A. Golovchenko: Ion-beam sculpting at nanometre length scales. *Nature* 412, 166-169 (2001)
18. Chen, P., T. Mitsui, D. B. Farmer, J. Golovchenko, R. G. Gordon & D. Branton: Atomic Layer Deposition to Fine-Tune the Surface Properties and Diameters of Fabricated Nanopores. *Nano Letters* 4, 1333-1337 (2004)
19. Chen, P., J. Gu, E. Brandin, Y.-R. Kim, Q. Wang & D. Branton: Probing single DNA molecule transport using fabricated nanopores. *Nano Letters* 4, 2293-2298 (2004)
20. Aksimentiev, A., J. B. Heng, G. Timp & K. Schulten: Microscopic kinetics of DNA translocation through synthetic nanopores. *Biophysical J.* 87, 2086-2097 (2004)
21. Yeh, I.-C. & G. Hummer: Nucleic acid transport through carbon nanotube membranes. *PNAS* 101, 12177-12182 (2004)
22. Heng, J. B., C. Ho, T. Kim, R. Timp, A. Aksimentiev, Y. V. Grinkova, S. Sligar, K. Schulten & G. Timp: Sizing DNA using a nanometer-diameter pore. *Biophysical J.* 87, 2905-2911 (2004)
23. Rant, U., K. Arinaga, T. Fujiwara, S. Fujita, M. Tornow, N. Yokoyama & G. Abstreiter: Excessive counterion condensation on immobilized ssDNA in solution of high ionic strength. *Biophysical J.* 85, 3858-3864 (2003)
24. Saenger, W., J. Riecke & D. Suck: A structural model for the polyadenylic acid single helix. *J. Mol. Biol.* 93, 529-534 (1975)
25. Watson, J. D. & F. H. Crick: Molecular structure of nucleic acids. *Nature* 171, 737-738 (1953)
26. Arnott, S., R. Chandrasekaran & A. G. W. Leslie: Structure of the single-stranded polyribonucleotide polycytidylic acid. *J. Mol. Biol.* 106, 735-748 (1976)
27. Muthukumar, M.: Polymer translocation through a hole. *Journal of Chemical Physics* 111, 10371-10374 (1999)
28. Fologea, D., M. Gershow, B. Ledden, D. S. McNabb, J. A. Golovchenko & J. Li: Detecting single stranded DNA with a solid state nanopore. *Nano Letters* 5, 1905-1909 (2005)

**Abbreviations:** ssDNA: single stranded DNA; dsDNA: double stranded DNA; ALD: atomic layer deposition; polydA: single stranded poly-deoxyadenosine; polydC: single stranded poly-deoxycytosine; dA100: poly-deoxyadenosine 100 mers; dC100: poly-deoxycytosine 100 mers.

**Key Words:** nanopore, bio-nanotechnology, DNA structure, single molecule detection, electrophoresis, Biosensor, nanofabrication

**Send correspondence to:** Dr. Peng Chen, Division of Bioengineering, School of Chemical & Biomedical Engineering, Nanyang Technological University, 70

Nanyang Drive, Singapore 637457, Tel: 65 6316 8879, Fax: 65 6791 1761, E-mail: chenpeng@ntu.edu.sg

<http://www.bioscience.org/current/vol12.htm>